JCTC Journal of Chemical Theory and Computation

Article

pubs.acs.org/JCTC

Treatment of Ionic Strength in Biomolecular Simulations of Charged Lipid Bilayers

Diogo Vila-Viçosa,[†] Vitor H. Teixeira,[†] Hugo A. F. Santos,[‡] António M. Baptista,[§] and Miguel Machuqueiro*,[†]

[†]Centro de Química e Bioquímica and Departamento de Química e Bioquímica, Faculdade de Ciências, Universidade de Lisboa, 1749-016 Lisboa, Portugal

[‡]Faculty of Sciences, BioFIG—Centre for Biodiversity, Functional and Integrative Genomics, University of Lisboa, 1649-004 Lisboa, Portugal

[§]Instituto de Tecnologia Química e Biológica, Universidade Nova de Lisboa, Av. da República, 2780-157 Oeiras, Portugal

Supporting Information

ABSTRACT: Biological membranes are complex systems that have recently attracted a significant scientific interest. Due to the presence of many different anionic lipids, these membranes are usually negatively charged and sensitive to pH. The protonation states of lipids and the ion distribution close to the bilayer are two of the main challenges in biomolecular simulations of these systems. These two problems have been circumvented by using ionized (deprotonated) anionic lipids and enough counterions to preserve the electroneutrality. In this work, we propose a method based on the Poisson−Boltzmann equation to estimate the counterion and co-ion concentration close to a lipid bilayer that avoids the need for neutrality at this microscopic level. The estimated number of ions was tested in molecular dynamics simulations of a 25% DMPA/DMPC lipid bilayer at different ionization levels. Our results show that the system neutralization represents an overestimation of the number of counterions. Consequently, the resulting lipid bilayer becomes too ordered and practically insensitive to ionization. On the other hand, our proposed approach is able to correctly model the ionization dependent isothermal phase transition of the bilayer observed experimentally. Furthermore, our approach is not too computationally expensive and can easily be used to model diverse charged biomolecular systems in molecular dynamics simulations.

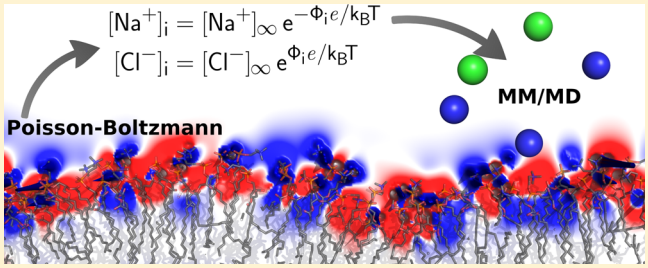

1. INTRODUCTION

Biological membranes are complex systems that have been broadly studied in recent years.[1−6] They possess a large variety of lipids, mainly neutral (zwitterionic) and anionic.[7] Most biological membranes are negatively charged and sensitive to pH. Consequently, their protonation state is altered upon small pH changes and can be related with many biological processes such as signal transduction.[1,8−13]

Membrane biophysical models, often used to understand the behavior of biological lipid bilayers, are usually simple and mainly composed of pure lipids and, in some cases, of binary or ternary mixtures.[14−16] Moreover, phosphatidylcholines (PC) are widely used to model membranes since, in general, they are the main component of eukaryotic biological membranes[17] and form very stable lipid bilayers.[2,3] In particular, 1,2-dimyristoyl-*sn*-glycero-3-phosphocholine (DMPC) is commonly used in theoretical models of lipid bilayers since it is well-parametrized in most biomolecular force fields,[5] and there is considerable structural information for its L_α lamellar phase.[2,3,18−31]

In the past decade, molecular dynamics (MD) simulations have been widely used to study lipid bilayers at the molecular level. To increase the realism of the model systems used in such simulations, it is crucial to add anionic lipids such as 1,2-dimyristoyl-*sn*-glycero-3-phosphate (DMPA). The phosphatidic acid (PA) family of phospholipids is particularly sensitive to pH at physiological levels and has an important role in the regulation of several biological processes,[12,32−35] such as in the Opi1 mediated control of phospholipid synthesis and lipid metabolism.[12]

The simulation of charged binary systems (such as DMPA/DMPC mixtures) poses two main challenges: first, the ionization of the bilayer strongly depends on pH and on the DMPA/DMPC ratio;[1] second, the ion distribution close to the membrane has a high impact on the membrane stability and depends on the membrane ionization and on the ionic strength of the solution. These two problems have been addressed by considering lipids to be ionized (deprotonated) and adding the corresponding amount of counterions needed to preserve the electroneutrality, with or without additional ions to describe the bulk ionic strength effect.[36−42] For this purpose, Particle Mesh Ewald (PME)[43] is commonly used to describe the long-range

Received: July 29, 2014
Published: October 30, 2014

   dx.doi.org/10.1021/ct500680q | *J. Chem. Theory Comput.* 2014, 10, 5483−5492

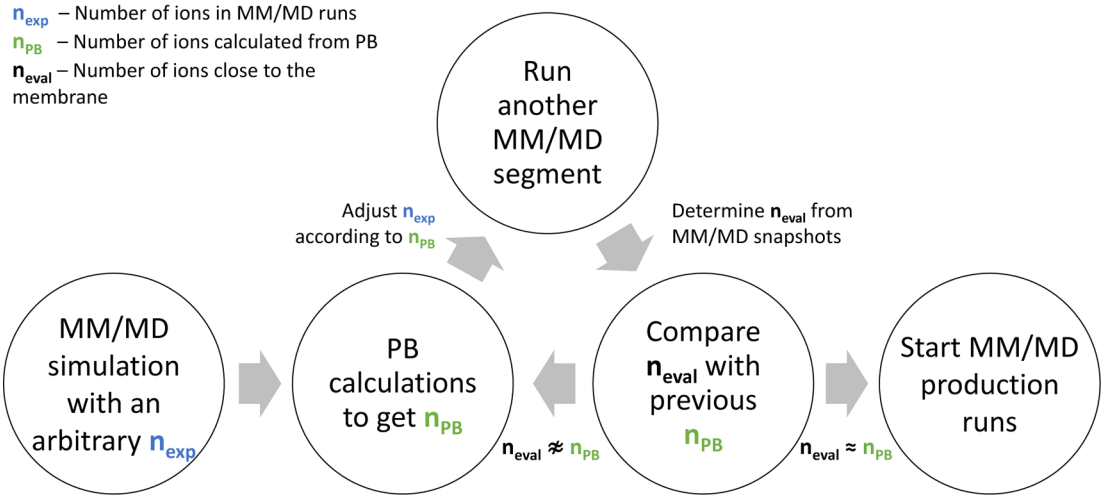

Figure 1. Workflow to calculate the final number of explicit ions obtained from the self-consistent procedure.

electrostatic interactions in MD simulations (see ref 44 for a recent review on the electrostatic treatment in MD simulations). However, the neutrality of the system might not be appropriate for a highly charged system at this microscopic scale. For example, according to Gouy–Chapman (GC) theory and Monte Carlo (MC) simulations, the concentration of counterions and co-ions close to a charged surface with a charge density $\sigma = -0.0621$ C m^{-2} (approximately 23% of singly charged lipids in a membrane with an average area per lipid of 0.6 nm) only converges to the bulk value of 0.1 M at ∼3 nm (see Figure 14.8 from ref 45). This means that, in these conditions, the electroneutrality is only achieved after this distance from the surface. Hence, to simulate a neutral system one would need to use a very large simulation box (in z direction) which would be too time-consuming. To avoid this, it is necessary to model the local effects of the ionic strength (that are strongly related with the electrostatic potential generated by the membrane) without introducing artifacts.

The Poisson–Boltzmann (PB) equation[42,46−49] (from which GC theory results[35,50] as a particular case) and MC simulations[51−53] have been widely used to describe the concentration profile of the ions (counterions and co-ions) close to a charged surface. Both GC and MC simulations of ions often ignore the molecular detail of the charged surface.[45] However, the numerically solved PB equation can be used to describe the potential (and consequently the ion distribution) close to a membrane with atomic detail.[42,45,46] This equation provides a mathematical relation between the charge distribution in a solute and the electrostatic potential generated by it in a continuous medium with a specific dielectric constant and salt concentration. This electrostatic potential can then be used to estimate the amount of ions close to the solute, in our case, a lipid bilayer (see the Theory and Methods section for details).

In this work, we propose a method based on the PB equation to estimate the counterion and co-ion concentration close to a lipid bilayer. The estimated number of ions is then explicitly included in a MD simulation of the system. We performed our simulations using a generalized reaction field (GRF)[54] to treat long-range electrostatic interactions and the bulk effect of ionic strength (instead of GRF, one might use PME with a neutralizing uniform background charge density, but such an approach was recently found to introduce artifacts in inhomogeneous systems[55]). We compared the results obtained using our method with simulations without any explicit ions and with neutralized systems simulated with both GRF and PME.

2. THEORY AND METHODS

2.1. Estimation of the Number of Explicit Ions. As stated in the Introduction, we use a PB model to estimate the amount of counterions and co-ions near a charged membrane. Given the variable size of the MD simulation box, together with the fact that the across-solvent distance between the two monolayers in the periodic box was always only slightly higher than twice the cutoff value used in the GRF treatment of long-range electrostatics (1.4 nm; see section 2.2.3), we decided to compute the amount of ions only up to such distance. This substantially simplifies the computational procedure and corresponds to differences of only tenths of an ion.

According to the Poisson–Boltzmann (PB) theory, the number density of an ion with charge z at position $\mathbf{r}$ is given by[45,46,56]

$$\rho(\mathbf{r}) = \rho_0 e^{-ze\phi(\mathbf{r})/k_B T} \quad (1)$$

where $\phi(\mathbf{r})$ is the electrostatic potential at $\mathbf{r}$, ρ_0 is the bulk number density, e is the elementary charge, k_B is the Boltzmann constant, and T is the absolute temperature. If we discretize the region C encompassed by the cutoff into a set of M small cells, each with volume V and approximately constant electrostatic potential, we obtain a PB-estimate of the total amount of ions of this type in region C:

$$n_{PB} = \int_C \rho(\mathbf{r})\, d\nu \approx V N_A I \sum_{i=1}^{M} e^{-ze\phi_i/k_B T} \quad (2)$$

where ϕ_i is the potential in cell i, and we used the fact that $\rho_0 = N_A I$ for a 1:1 salt, where N_A is Avogadro's constant and I is the solution ionic strength. This equation is then used to calculate the number of cations, $n_{PB}(A^+)$, and of anions, $n_{PB}(Cl^-)$, for each of a set of conformations from a MD simulation. The median, which is robust to outliers, of these calculated values is then used as an estimation for the next MD simulation of the same system.

The workflow to calculate the final number of explicit ions ($n_{exp}(A^+)$ and $n_{exp}(Cl^-)$) is represented in Figure 1. The first

dx.doi.org/10.1021/ct500680q | J. Chem. Theory Comput. 2014, 10, 5483−5492

MM/MD simulation is performed by setting n_{exp} to any number within 0 and enough ions for neutralization of the system (this initial guess does not affect the final converged result). After this first simulation, the n_{PB} values are calculated as explained above and n_{exp} are adjusted accordingly. We then determine the number of explicit ions that are closer than 1.4 nm to the membrane in the new set of conformations ($n_{eval}(A^+)$ and $n_{eval}(Cl^-)$). After the calculation of both n_{PB} and n_{eval} the two pairs of values are compared and, if necessary, n_{exp} is adjusted for a new MD simulation. This process continues iteratively until $n_{eval} \approx n_{PB}$, i.e. the process becomes self-consistent (usually after 2 or 3 iterations).

2.2. Methods. *2.2.1. Simulations Setup.* All simulated systems were composed of 128 lipids, 32 DMPA, and 96 DMPC molecules equally distributed by the two monolayers (representing 25% of DMPA and 75% of DMPC). The phosphate group of DMPC was kept deprotonated (zwitter-ionic lipid) in all simulations. In the case of DMPA, whose headgroup has three possible protonation states (with charge 0, −1, or −2 corresponding to double protonated, single protonated, and deprotonated, respectively), the ionization state was varied from 0 to −64 (see the Supporting Information for the used ionization states distributions). We performed simulations with both GRF and PME treatment for long-range electrostatic interactions (Table 1). Both Na^+ and K^+ were used as counterions and Cl^- was used as co-ion in all simulations. In PB^{NaCl} and PB^{KCl}, the number of ions were calculated according to the methodology described in section 2.1, while the remaining simulations used either sufficient counterions to neutralize the system (GRF^{Na}, GRF^{K}, PME^{Na}, and PME^{K}) or none ($GRF^{no\text{-}ions}$). The number of water molecules were adjusted to maintain a similar size of water region beyond the 1.4 nm cutoff for all systems (around 150 molecules).

Table 1. Summary of the Simulations Performed in This Work[a]

name	electrostatics	counterion	co-ion	system charge
PB^{NaCl}	GRF	Na^+	Cl^-	Variable[b]
GRF^{Na}	GRF	Na^+		0
PME^{Na}	PME	Na^+		0
PB^{KCl}	GRF	K^+	Cl^-	variable[b]
GRF^{K}	GRF	K^+		0
PME^{K}	PME	K^+		0
$GRF^{no\text{-}ions}$	GRF			membrane charge

[a]The bilayer ionization studied were 0, −16, −32, −48, and −64. GRF was always used with a fixed 0.1 M ionic strength. All simulations were done in triplicate for 100 ns each. [b]Depends on the number of ions calculated with our self-consistent methodology (see Results and Discussion).

2.2.2. Parametrization of Atomic Charges of DMPC and DMPA. The atomic partial charges for DMPC were taken from the work of Teixeira et al.[6] For the DMPA molecules the atomic partial charges for neutral, single ionized, and double ionized forms were calculated using a similar procedure: the geometries were optimized with Gaussian 03[57] at the HF/6-31G(d) level, and the resulting electrostatic potential was fitted to atomic coordinates using RESP[58] with P partial charge fixed to the Mulliken charge. The obtained charges were slightly adjusted to be consistent with the charge groups of the GROMOS96 54A7 force field (see the Supporting Information).

2.2.3. MM/MD. Molecular mechanics/dynamics (MM/MD) simulations were done with the GROMOS 54A7 force field[59] and a modified version[60,61] of GROMACS distribution (version 4.0.7[62,63]). The Lennard-Jones parameters for K^+ were taken from ref 64. The membrane was solvated in a tetragonal box with SPC water molecules,[65] with the membrane plane oriented parallel to the x and y axis. All lipid bond-lengths were constrained using the parallel version of the LINCS algorithm,[66] and the SETTLE algorithm[67] was used for water. The simulations were done in the NPT ensemble, using the v-rescale thermostat[68] at 310 K with separate couplings for the solute and solvent (including ions, when present) with a relaxation time of 0.1 ps. A semi-isotropic Berendsen[69] pressure couple was used to maintain the pressure constant at 1 bar with a compressibility of 4.5×10^{-5} bar^{-1} and a relaxation time of 5.0 ps. An integration step of 2 fs was used in the equations of motion in all MD simulations.

Nonbonded interactions were treated with a twin-range method, using group-based cutoffs of 0.8 and 1.4 nm, updated every 5 steps. Long-range electrostatics were corrected with a GRF,[54,61] using a dielectric constant of 54.0[70] and an ionic strength of 0.1 M.[61] The Particle Mesh Ewald (PME) method[43] was also used in two sets of simulations. For this method, we used a grid spacing of 0.12 nm, the short-range interactions were computed using a nonbonded pairlist with a single cutoff of 1.0 nm, updated every 10 steps.

The minimization procedure consisted in three sequential steps: starting with up to 10 000 steps using the steepest descent algorithm (unconstrained), followed by 10 000 steps using the low-memory Broyden−Fletcher−Goldfarb−Shanno integrator (unconstrained), and ended with ∼300 steps using the steepest descent algorithm (with all bonds constrained).

The same initialization procedure was applied for all systems and consisted of four steps. First, a 50 ps MD simulation with all heavy atoms harmonically restrained with a force constant of 1000 kJ mol^{-1} nm^{-2}. In the three following steps of 100, 150, and 200 ps MD simulations, position restraints were applied differently for the phosphorus and remaining heavy atoms with force constants of 1000, 100, and 10 kJ mol^{-1} nm^{-2} and of 100, 10, and 0 kJ mol^{-1} nm^{-2}, respectively. The MD simulations of all bilayer systems were pre-equilibrated for 100 ns, after which three replicates were done for an additional 100 ns.

2.2.4. Ion Estimation Using a Poisson−Boltzmann Model. The Poisson−Boltzmann (PB) calculations were done with the DelPhi software V5.1[71,72] using atomic radii taken from GROMOS 54A7 force field[59] and atomic partial charges as described in the previous sections. The molecular surface of the membrane was defined by a spherical probe of radius 0.14 nm, the ion exclusion layer was 0.2 nm, and the ionic strength was 0.1 M. The dielectric constant of the solvent was 80 and for the membrane we used a value of 2 (similar results were obtained with dielectric constant values between 2 and 8). Considering the membrane oriented along the xy plane, we explicitly applied PBC along the x and y directions. The convergence threshold value based on maximum change of potential was set to 0.01. In the iteration convergence process, we used relaxation parameters for both nonlinear and linear forms of the PB equation with values of 0.15 and 0.20. The PB calculations were performed in a cubic (finite differences) grid with 251 points per side (corresponding to a grid space of ∼0.05 nm). For these calculations were used 200 conformations from each PB^{NaCl} and PB^{KCl} simulation.

Table 2. Number of Ions in PB^{NaCl} and PB^{KCl} simulations

		n_{exp}		n_{eval}		n_{PB}		n_{GC}			
counterion	lipid charge	A^{+b}	Cl^-	A^+	Cl^-	A^+	Cl^-	A^+	Cl^-	system charge	neval(A^+) − $n_{eval}(Cl^-)^a$
Na^+	0	5	7	5.0	6.3	4.6	6.7			−2	−1.3
	−16	6	7	6.0	6.3	5.9	7.1	15.4	2.6	−17	−0.3
	−32	8	7	8.0	6.0	7.4	7.0	28.8	2.0	−31	2.0
	−48	10	7	10.0	6.0	9.5	6.9	43.3	1.8	−45	4.0
	−64	12	7	12.0	5.4	12.7	6.7	58.3	1.7	−59	6.6
K^+	0	5	7	5.0	6.4	4.7	7.0			−2	−1.4
	−16	6	7	6.0	6.2	5.8	7.0	15.4	2.7	−17	−0.2
	−32	8	7	8.0	5.9	7.1	6.8	28.8	1.9	−31	2.1
	−48	10	7	10.0	5.6	9.2	6.6	43.4	1.7	−45	4.4
	−64	12	7	12.0	4.9	12.3	6.7	58.3	1.7	−59	7.1

[a]Average charge within the solvent region up to 1.4 nm from the membrane. [b]A^+ stands for either Na^+ or K^+.

To estimate the number of ions (n_{PB}), the electrostatic potential (ϕ) of the system is written to a new 3D grid with 50 points per side ($grid^{ion}$) and the same size as the finite difference grid. Different number of points per side were tested and consistent results were obtained using between 50 and 80 points. Using eq 2, we sum the number of ions n for all $grid^{ion}$ points whose shortest distance to any atom of the bilayer is larger than r_i + 0.2 nm and shorter than R_c, where r_i is the radii of the atom in the bilayer, 0.2 nm is the ion exclusion layer, and R_c = 1.4 nm, the GRF cutoff.

2.2.5. Calculation of Lipid Protonation. The lipid protonation was computed using a PB/MC methodology previously described.[6] PB calculations (with DelPhi V5.1[71,72]) were done in a cubic grid with 61 points per side and a two step focusing[73] where the focus grid was one-fourth of the coarser grid size. Since the dimension of the box changes along the simulation (the conformations were taken from the MD simulations, performed in NPT), the space between grid points for the coarser grid needs to be calculated for every conformation (average values around 0.1 and 0.025 nm for the coarse and focus grids, respectively). In the coarse grid, we used relaxation parameters of 0.2 and 0.75 for linear and nonlinear iteration convergence process. A cutoff of 2.5 nm was used to calculate the background and pairwise interactions (see ref 6 for more details). The pK_a values of the model compounds used were 1.29 for DMPC (the pK_a value of dimethylphosphate) and 1.54 and 6.31 for DMPA (the two pK_a values of methylphosphate).[74] Conformations for the protonation calculations were taken from the MD simulations from the equilibrated last 90 ns of each system at intervals of 10 ns. This makes 10 frames per replicate and a total of 30 for each system.

These calculations were performed in several configurations with mixtures of lipids in different protonation states, meaning that they are necessarily biased toward those inherited protonation states, similarly to what happens in linear response approximation calculations.[6,75,76] These limitations are usually circumvented with an increased dielectric constant value, in order to roughly account for the reorganization that would result from ionization changes. Therefore, based on our previous linear response approximation studies using a similar methodology,[6,76] dielectric constants of 8 and 80 were used for the membrane and the solvent, respectively. For a more detailed discussion on this subject, see refs 6 and 75−81.

The MC sampling was performed with the PETIT program[82] version 1.6.1 using an absolute temperature of 310 K. All runs were performed using 10^5 MC cycles, where one cycle consists of sequential state changes over all individual sites and pairs of sites with an interaction larger than 2 pH units.

2.2.6. Analyses. The last 90 ns of each simulation were used for analyses. Area per lipid (A_l) and deuterium order parameters were obtained using several tools from the GROMACS software package.[62,63] Membrane thickness and ion distributions were calculated using in-house tools. Membrane thickness was defined as twice the average z distance between each phosphorus atom and the center of mass (also in z) of all phosphorus atoms. All presented errors were computed using standard methods based on the autocorrelation function of the property measured to determine the number of independent blocks in the simulations.[83]

3. RESULTS AND DISCUSSION

3.1. Ion Estimation. PB^{NaCl} and PB^{KCl} simulations were performed with a variable number of ions that were calculated according to the method described in section 2.1 (see Table 2 and Figure 2). In these two groups of simulations the number of counterions (Na^+ or K^+) varied between 5 and 12 and the number of co-ions (Cl^-) was 7 in all simulations, i.e. the number of co-ions is almost insensitive to the membrane ionization while the number of counterions always increases with the membrane charge. This is expected since there is usually an accumulation of counterions close to a charged surface (following a Boltzmann distribution—see Theory and Methods). Since the ionization of DMPA varies between 0 and −64, these small number of ions lead to systems with total charges between −2 and −59. Consequently, according to our

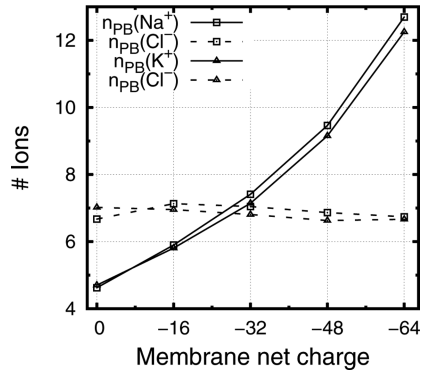

Figure 2. Number of counterions ($n_{PB}(A^+)$) and co-ions ($n_{PB}(Cl^-)$) in PB^{NaCl} and PB^{KCl} simulations according to the PB-based methodology.

methodology, a microscopic system with the size of our simulation box (~7−8 nm in z direction) is not globally neutral. In particular, the PB^{NaCl} system with 64 negative charges requires 12 Na^+ and 7 Cl^- closer than 1.4 nm, an example particularly far from neutrality. Nevertheless, all membranes were stable during our simulations, without any disruptions. From our results, we can also observe that the number of predicted Na^+ and K^+ is the same in their corresponding simulations. This suggests that these two ions have similar counterion behaviors regardless of their chemical nature and preferred membrane interaction regions. Another nonintuitive result is that the neutral system requires slightly more Cl^- co-ions than counterions. This observation can be explained by the positively charged layer that is generated in our model by the choline groups of DMPC that can be partially stabilized by the presence of negative ions. However, confirmation of this result would require a robustness analysis (e.g., using different force field parameters), which falls outside the scope of this work. Once again, system neutrality is only achieved farther from this distance from the surface. Table 2 also shows the ion estimation using a GC model (n_{GC}; see the Supporting Information). The estimated number of cations is larger than n_{PB}, indicating that the lack of molecular detail is overestimating these values. These results illustrate the need to use PB for these calculations instead of the more simplified and computationally inexpensive GC approach.

3.2. Isothermal Phase Transition. The area per lipid (A_l) values were calculated for PB^{NaCl} and PB^{KCl} simulations (Figure 3) by averaging along 270 ns for each system (last 90 ns of each replicate). When the membrane is neutral, the repulsion between the head groups is minimized and the A_l is very low corresponding to the gel phase of pure DMPC (see blue marked region in Figure 3). As we increase the ionization of the bilayer, the A_l also increases, which is not surprising since the electrostatic repulsion between the head groups is stronger. In the simulations with 32 and 48 negative charges, the A_l is in the range of fluid DMPC[2,3,18−25] (see red marked region in Figure 3), while above 48 the values exceed this region (0.65 nm^2). With these results, we were able to model an isothermal gel−fluid phase transition in our membrane that is only associated with changes in the ionization state of the DMPA. Additionally, according to the average A_l of our systems, Na^+ and K^+ have a similar impact on our bilayer. Probably, the role of the counterions in our systems is mainly electrostatic and the chemical nature of the ion (Lennard−Jones parameters) plays a secondary role in this property. In fact, the A_l in systems with K^+ is always a bit smaller that the ones with Na^+. The smaller radius of Na^+ allows it to interact with the lipids in the ester region while K^+ stays a little above in the phosphate region minimizing the repulsion between them (see the next section for further structural information).

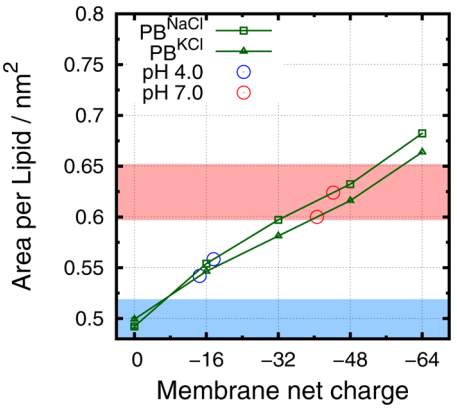

Figure 3. Average area per lipid (A_l) of PB^{NaCl} and PB^{KCl} simulations as a function of the membrane net charge. Typical experimental values ranges for gel and liquid crystalline phases of DMPC are marked in blue and red, respectively.[2,3,18−25] The ionization estimated for pH 4 and 7 are also plotted.

The pseudobinary phase diagrams for the DMPA/DMPC mixture at several pH values has been previously reported.[1] It was shown that, at pH 7 and T = 310 K, the 25% DMPA/DMPC mixture is in a fluid phase. At the same temperature but at pH 4, the mixture is in a gel + fluid phase state and, in some conditions, a macroscopic phase separation is observed. In our simulations, these behaviors occur when the ionization is −48 (fluid phase that is typical of pH 7) and when it is −16 (intermediate phase that may be typical of pH 4). To gain insight into the agreement of our results with the experiment, we performed PB/MC calculations to determine the pH at which the ionization is the same as in the simulation (see the Supporting Information). Since the conformations were sampled at the given protonation states, the obtained pH values are extracted from the most reliable regions of the total titration curves. With these pH values, we were able to linearly interpolate the ionization at pH 4.0 and 7.0 (Table 3 and the Supporting Information). These results show that the A_l obtained with our methodology is in excellent agreement with the lipid phases experimentally observed.[1]

Table 3. Estimated Ionization at pH 4.0 and 7.0 from PB^{NaCl} Simulations

pH	Na^+	K^+
4	−17.6	−14.5
7	−44.2	−40.6

In order to compare the presented methodology with commonly used approaches, we performed five additional sets of simulations (see Theory and Methods) with both GRF and PME. It was used a set of systems without explicit addition of ions leaving the ionic screening to the long-range electrostatic treatment of GRF with I = 0.1 M ($GRF^{no\text{-}ions}$). We also performed simulations with neutral systems and, in these cases, both GRF with I = 0.1 M (GRF^{Na}, GRF^{K}) and PME (PME^{Na}, PME^{K}) were employed. Figure 4 shows the A_l per ionization for all these systems using both Na^+ and K^+ counterions. In the $GRF^{no\text{-}ions}$ system the A_l is strongly dependent on the ionization of the bilayer. It varies between a gel-like phase (with $A_l \sim 0.5$ nm^2) and a very fluid phase ($A_l > 0.75$ nm^2) where the membrane is significantly distorted. In these simulations, due to the absence of counterions, the repulsion between the negatively charged head groups is very high, being only attenuated by an implicit ionic strength screening. At pH 7.0, the obtained A_l (0.67 nm^2) reflects the excessive destabilization present in this set of simulations. This result shows that, when dealing with significantly charged lipid bilayers, the use of counterions is essential. In the neutral systems (GRF^{Na}, GRF^{K}, PME^{Na} and PME^{K}) the A_l curves are not significantly affected by the ionization. This can be explained by the counterions sequestration to the membrane that occur in the systems where they are available. Therefore, the number of stabilizing counterions is probably in excess since, independently of the

dx.doi.org/10.1021/ct500680q | J. Chem. Theory Comput. 2014, 10, 5483−5492

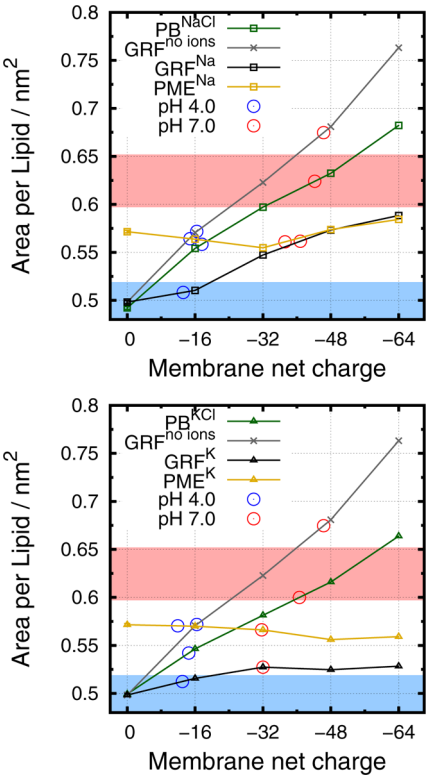

Figure 4. Average area per lipid (A_l) for all simulated systems as a function of the membrane net charge using either Na^+ (top panel) or K^+ (bottom panel) as counterions. Simulations with Na^+ as counterion in the top panel and with K^+ in bottom. Typical experimental values ranges for gel and liquid crystalline phases of DMPC are marked in blue and red, respectively.[2,3,18−25] The ionization estimated for pH 4 and 7 are also plotted.

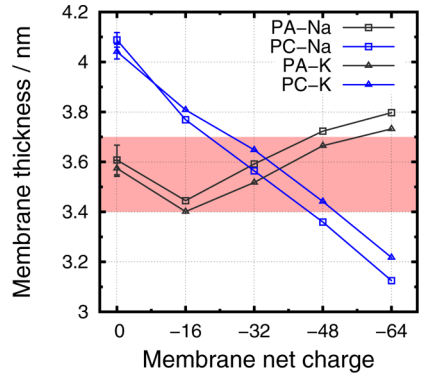

Figure 5. Average membrane thickness of PB^{NaCl} and PB^{KCl} simulations as a function of membrane net charge. Typical experimental values range for liquid crystalline phase of DMPC is shown in red.[84]

counterion and the long-range electrostatics treatment method used, the membrane is never observed in the fluid phase as expected from experiment.[1] Recently, it has also been observed that a charged membrane moiety rigidifies in an electroneutral system.[42]

These results show that the neutrality is inadequate to describe this charged lipid bilayer and its close vicinity as it is usually modeled in MD simulations. On the other hand, with our method the system is usually far from neutrality but is able to correctly model the isothermal phase transition observed in this DMPA/DMPC pseudobinary system.[1]

3.3. Structural Analysis. Membrane thickness is a very helpful structural property, specially when using lipid mixtures since it allows to easily discriminate between the different species. Also, this property can be a good descriptor of the lipid phase transition. Figure 5 shows the membrane thickness in the PB^{NaCl} and PB^{KCl} simulations calculated separately for DMPA and DMPC. Interestingly, even though the ionization is centered on the DMPA molecules, we observe a clear phase transition only on DMPC. It seems that protonation of DMPA induces a better packing of the DMPC molecules increasing its thickness from values typical of a fluid phase (3.4−3.7 nm[84]) to values up to ∼4.1 nm which are probably only observed in more ordered phases. The membrane thickness of DMPA is less sensitive to its ionization and its increase is probably related with the high solvent exposure needed to stabilize its ionized form. As a consequence, DMPC is driven to sample rather lower thickness values (∼3.2 nm).

Deuterium order parameter is also a widely used structural property of lipid bilayers that can easily aid on the discrimination of its constituents. With this property, we follow the phase transition focusing on the packing of the lipid tails. Figure 6 shows the order parameters calculated for the PB^{NaCl} and PB^{KCl} simulations. Both DMPA and DMPC molecules show an ionization dependence of the order parameter. However, while DMPC packs more gradually as the membrane ionization decreases, DMPA lipid tails are kept mostly disordered in the ionized systems, only becoming ordered upon full protonation. As observed for the membrane thickness, DMPC is the lipid more sensitive to the phase transition. Once again, at ionization of −48 the S_{CD} values for the plateau region of DMPC (methylene groups 3−6) are within the experimental range for a pure DMPC bilayer (0.17−0.21[29]).

According to both the membrane thickness and deuterium order parameters, there are no significant differences between using Na^+ or K^+ as counterions in our systems. To better understand the different roles of these counterions, we calculated the counterion distribution around oxygen atoms of phosphates and ester carbonyl groups for both PB^{NaCl} and PB^{KCl} simulations (Figure 7). These results clearly show that the counterions are interacting with different regions of the lipids. The smaller Na^+ ions are able to insert into deeper regions of the bilayer interacting preferentially with the ester groups (peak at ∼0.23 nm). The larger K^+ ions are excluded from these regions and, consequently, remain at a more shallow region interacting preferentially with the phosphate groups (peak at ∼0.25 nm). With increasing ionization, we observe the gradual release of Na^+ which can be triggered by the increase of membrane fluidity promoting the solvent exposure of the ester regions. On the contrary, the normalized number of K^+ ions interacting with its preferred partners (phosphate groups) does not depend on the ionization, suggesting that this counterion is strongly attached to the membrane. Moreover, there are recent evidences that the current Na^+ ion MM parameters might lead to an overbinding of this ion to PC bilayers.[41,85] Regardless of these apparent shortcomings in their parametrizations, both ions were able to correctly stabilize the charged lipid bilayers to similar extents, which indicates that the electrostatic counterion effect overcomes their preferred membrane interaction regions.

4. CONCLUSIONS

Here, we present a method to estimate the number of ions close to a charged lipid bilayer at a given ionic strength. This

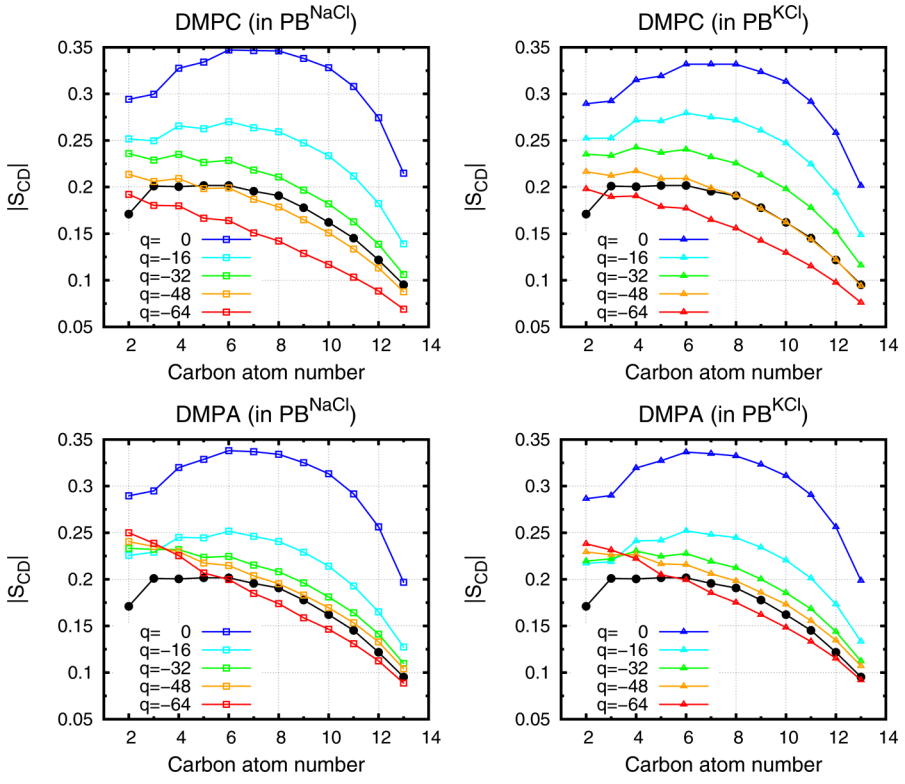

Figure 6. Deuterium order parameters for PB^{NaCl} and PB^{KCl} simulations. Experimental curve for DMPC in the liquid crystalline phase is shown in black circles. These values were linearly interpolated to the desired temperature (310 K) from the three available temperature sets (303, 323, and 338 K).[29]

method is proposed as an alternative to the commonly used approaches based on system neutrality.[36−42] It has been shown that the electrostatic potential generated by a charged surface is propagated over large z direction distances beyond the commonly used MD system sizes.[35,45−48,50−53] Therefore, at this microscopic level the system neutrality does not seem appropriate.

Our results show that the system neutralization of an ionized PA/PC bilayer represents an overestimation of the number of counterions. Consequently, the resulting lipid bilayer becomes too ordered and practically insensitive to ionization. A similar observation has been recently made where it was shown that the membrane moiety gets rigidified in an electroneutral system.[42] On the other hand, with our method, we were able to correctly model the ionization dependent isothermal phase transition of a 25% PA/PC bilayer.[1] This transition was observed following several structural properties usually used to describe lipid bilayers, namely area per lipid (A_l), deuterium order parameters, and membrane thickness.

We also compared two treatments of the long-range electrostatics: PME and GRF. Using these two approaches in neutral systems, we observed similar and almost ionization insensitive behaviors in terms of A_l. It has been shown that PME in inhomogeneous systems (such as a bilayer-water mixture) with a system net charge leads to significant artifacts,[55] rendering this approach inappropriate to model such small and charged systems.

GRF was also tested without any ions and we were able to observe a significant ionization dependent isothermal transition. However, in this group of simulations, the observed A_l values are too large for a typical fluid phase of DMPC and the ionization at which the transition occurs is not in complete agreement with the experimental data.[1] These results indicate that the "reaction field" approach alone does not stabilize enough a bilayer system with a large net charge.

The MD parameters of ions are difficult to obtain and have been the subject of several works in recent years.[59,64] Despite such efforts, it has been shown that the Na^+ parameters used in this work might lead to an overbinding of this ion to the lipid bilayer.[41,85] To circumvent these limitations, we performed our simulations with both Na^+ and K^+ as counterions. Interestingly, these ions have different preferential regions of interaction with the lipid molecules: Na^+ prefers to interact at deeper regions near the ester groups, while K^+ stays in a more shallow region close to the phosphates probably due to its larger size. However, with both ions the membranes showed similar behaviors in terms of all structural properties. Therefore, the role as electrostatic counterions is their most relevant effect, overcoming the artifacts that may arise from the MM description.

A PB-based approach to estimate the counterions distribution close to a charged surface can be considered a rough approximation. However, with this method, there is a good description of the heterogeneous charge distribution and the roughness of the membrane surface. Furthermore, our approach is not too computationally expensive and can easily be relevant to model diverse charged biomolecular systems in MD simulations. In the future, this method can also be very important to study several pH-dependent events using the so-called constant-pH MD methodologies.[60,61,86−105]

dx.doi.org/10.1021/ct500680q | J. Chem. Theory Comput. 2014, 10, 5483−5492

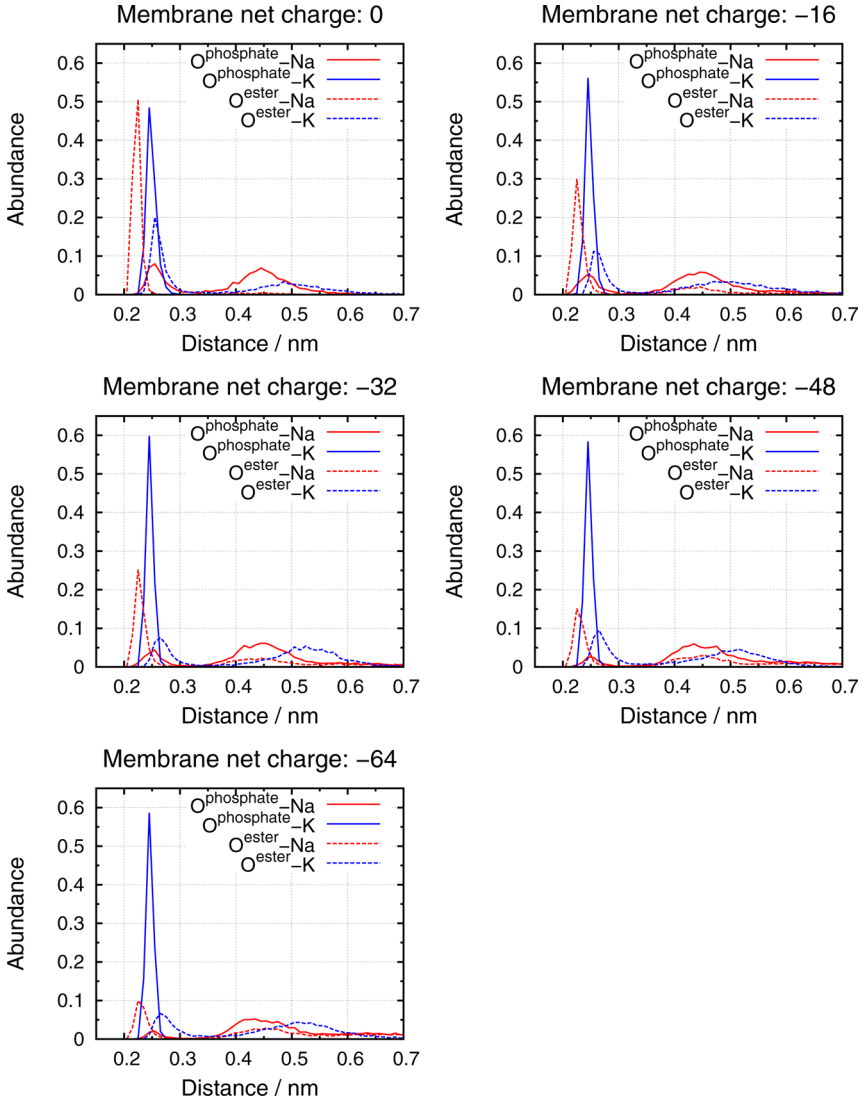

Figure 7. Minimum distance histograms for counterions relatively to O atoms of phosphates and esters (for PB^{NaCl} and PB^{KCl} simulations), normalized by the number of ions.

■ ASSOCIATED CONTENT

Supporting Information

Table with the ionization states distribution in the studied membranes. Image and table with the partial atomic charges of the three protonation states of DMPA. Procedure to deterimine the number of ions from GC theory and the ionization at pH 4.0 and 7.0 in all simulations. This material is available free of charge via the Internet at http://pubs.acs.org/.

■ AUTHOR INFORMATION

Corresponding Author

*E-mail: machuque@fc.ul.pt. Phone: +351-21-7500112. Fax: +351-21-7500088.

Notes

The authors declare no competing financial interest.

■ ACKNOWLEDGMENTS

We thank Maria J. Calhorda, Paulo J. Costa, João Henriques, and Sara R. R. Campos for fruitful discussions. We acknowledge financial support from Fundação para a Ciência e a Tecnologia through projects PTDC/QUI-BIQ/113721/2009, PTDC/QEQ-COM/1623/2012 and PEst-OE/QUI/UI0612/2013 and grant SFRH/BD/81017/2011.

■ REFERENCES

(1) Garidel, P.; Johann, C.; Blume, A. *Biophys. J.* **1997**, *72*, 2196−2210.
(2) Nagle, J. F.; Tristram-Nagle, S. *Curr. Opin. Struct. Biol.* **2000**, *10*, 474−480.
(3) Nagle, J.; Tristram-Nagle, S. *Biochem. Biophys. Acta* **2000**, *1469*, 159−195.
(4) Haines, T. H. *Biochem. Biophys. Acta, Biomembr.* **2009**, *1788*, 1997−2002.
(5) Poger, D.; Mark, A. E. *J. Chem. Theory Comput.* **2010**, *6*, 325−336.
(6) Teixeira, V. H.; Vila-Viçosa, D.; Baptista, A. M.; Machuqueiro, M. *J. Chem. Theory Comput.* **2014**, *10*, 2176−2184.
(7) Nelson, D. L.; Cox, M. M. *Lehninger Principles of Biochemistry*; WH Freeman and Company: New York, NY, 2005; pp 343−420.
(8) Träuble, H.; Eibl, H. *Proc. Natl. Acad. Sci. U.S.A.* **1974**, *71*, 214−219.
(9) Loewen, C. J. R.; Gaspar, M. L.; Jesch, S. A.; Delon, C.; Ktistakis, N. T.; Henry, S. A.; Levine, T. P. *Science* **2004**, *304*, 1644−1647.
(10) Wang, X.; Devaiah, S. P.; Zhang, W.; Welti, R. *Prog. Lipid Res.* **2006**, *45*, 250−278.

(11) Young, B. P.; Shin, J. J. H.; Orij, R.; Chao, J. T.; Li, S. C.; Guan, X. L.; Khong, A.; Jan, E.; Wenk, M. R.; Prinz, G. J.; William, A. S.; Loewen, C. J. R. *Science* **2010**, *329*, 1085−1088.
(12) Shin, J. J. H.; Loewen, C. J. R. *BMC Biol.* **2011**, *9*, 85.
(13) Loew, S.; Kooijman, E. E.; May, S. *Chem. Phys. Lipids* **2013**, *169*, 9−18.
(14) Tieleman, D. P.; Marrink, S.-J.; Berendsen, H. J. *Biochem. Biophys. Acta, Rev. Biomembr.* **1997**, *1331*, 235−270.
(15) Menger, F. M.; Chlebowski, M. E.; Galloway, A. L.; Lu, H.; Seredyuk, V. A.; Sorrells, J. L.; Zhang, H. *Langmuir* **2005**, *21*, 10336−10341.
(16) Van Meer, G.; Voelker, D. R.; Feigenson, G. W. *Nat. Rev. Mol. Cell. Bio.* **2008**, *9*, 112−124.
(17) de Kroon, A. I. *Biochem. Biophys. Acta* **2007**, *1771*, 343−352.
(18) Nagle, J. F.; Wilkinson, D. A. *Biophys. J.* **1978**, *23*, 159−175.
(19) Janiak, M.; Small, D.; Shipley, G. *J. Biol. Chem.* **1979**, *254*, 6068−6078.
(20) Lis, L.; McAlister, M.; Fuller, N.; Rand, R.; Parsegian, V. *Biophys. J.* **1982**, *37*, 657.
(21) Lewis, B. A.; Engelman, D. M. *J. Mol. Biol.* **1983**, *166*, 211−217.
(22) Rand, R.; Parsegian, V. *Biochem. Biophys. Acta* **1989**, *988*, 351−376.
(23) Koenig, B.; Strey, H.; Gawrisch, K. *Biophys. J.* **1997**, *73*, 1954−1966.
(24) Petrache, H.; Tristram-Nagle, S.; Nagle, J. *Chem. Phys. Lipids* **1998**, *95*, 83−94.
(25) Kučerka, N.; Liu, Y.; Chu, N.; Petrache, H.; Tristram-Nagle, S.; Nagle, J. *Biophys. J.* **2005**, *88*, 2626−2637.
(26) De Young, L. R.; Dill, K. A. *Biochemistry* **1988**, *27*, 5281−5289.
(27) Smaby, J. M.; Momsen, M. M.; Brockman, H. L.; Brown, R. E. *Biophys. J.* **1997**, *73*, 1492−1505.
(28) Costigan, S.; Booth, P.; Templer, R. *Biochem. Biophys. Acta, Biomembr.* **2000**, *1468*, 41−54.
(29) Petrache, H.; Dodd, S.; Brown, M. *Biophys. J.* **2000**, *79*, 3172−3192.
(30) Balgavỳ, P.; Dubničková, M.; Kučerka, N.; Kiselev, M. A.; Yaradaikin, S. P.; Uhríková, D. *Biochem. Biophys. Acta, Biomembr.* **2001**, *1512*, 40−52.
(31) Kučerka, N.; Kiselev, M. A.; Balgavỳ, P. *Eur. Biophys. J.* **2004**, *33*, 328−334.
(32) Eibl, H.; Blume, A. *Biochem. Biophys. Acta, Biomembr.* **1979**, *553*, 476−488.
(33) Blume, A.; Tuchtenhagen, J. *Biochemistry* **1992**, *31*, 4636−4642.
(34) Kooijman, E. E.; Tieleman, D. P.; Testerink, C.; Munnik, T.; Rijkers, D. T.; Burger, K. N.; de Kruijff, B. *J. Biol. Chem.* **2007**, *282*, 11356−11364.
(35) Mengistu, D. H.; Kooijman, E. E.; May, S. *Biochem. Biophys. Acta, Biomembr.* **2011**, *1808*, 1985−1992.
(36) Li, Z.; Venable, R. M.; Rogers, L. A.; Murray, D.; Pastor, R. W. *Biophys. J.* **2009**, *97*, 155−163.
(37) Pöyry, S.; Róg, T.; Karttunen, M.; Vattulainen, I. *J. Phys. Chem. B* **2009**, *113*, 15513−15521.
(38) Cordomí, A.; Prades, J.; Frau, J.; Vögler, O.; Funari, S. S.; Perez, J. J.; Escribá, P. V.; Barceló, F. *J. Lipid Res.* **2010**, *51*, 1113−1124.
(39) Lähdesmäki, K.; Ollila, O. H.; Koivuniemi, A.; Kovanen, P. T.; Hyvönen, M. T. *Biochem. Biophys. Acta, Biomembr.* **2010**, *1798*, 938−946.
(40) Yang, H.; Xu, Y.; Gao, Z.; Mao, Y.; Du, Y.; Jiang, H. *J. Phys. Chem. B* **2010**, *114*, 16978−16988.
(41) Venable, R. M.; Luo, Y.; Gawrisch, K.; Roux, B.; Pastor, R. W. *J. Phys. Chem. B* **2013**, *117*, 10183−10192.
(42) Dias, R. P.; Li, L.; Soares, T. A.; Alexov, E. *J. Comput. Chem.* **2014**, *35*, 1418−1429.
(43) Darden, T.; York, D.; Pedersen, L. *J. Chem. Phys.* **1993**, *98*, 10089−10092.
(44) Cisneros, G. A.; Karttunen, M.; Ren, P.; Sagui, C. *Chem. Rev.* **2014**, *114*, 779.
(45) Israelachvili, J. N. *Intermolecular and surface forces*, revised third ed.; Academic press, 2011; pp 291−340.
(46) Andelman, D. *Handbook of biological physics*; Elsevier, 1995; Vol. *1*, pp 603−642.
(47) Peitzsch, R. M.; Eisenberg, M.; Sharp, K. A.; McLaughlin, S. *Biophys. J.* **1995**, *68*, 729−738.
(48) Smart, J. L.; McCammon, J. A. *J. Am. Chem. Soc.* **1996**, *118*, 2283−2284.
(49) Lamm, G. *Rev. Comp. Ch.* **2003**, *19*, 147−333.
(50) Lakhdar-Ghazal, F.; Tichadou, J.-L.; Tocanne, J.-F. *Eur. J. Biochem.* **1983**, *134*, 531−537.
(51) Torrie, G. M.; Valleau, J. P. *Chem. Phys. Lipids* **1979**, *65*, 343−346.
(52) Jönsson, B.; Wennerstroem, H.; Halle, B. *J. Phys. Chem.* **1980**, *84*, 2179−2185.
(53) Guldbrand, L.; Jönsson, B.; Wennerström, H.; Linse, P. *J. Chem. Phys.* **1984**, *80*, 2221−2228.
(54) Tironi, I. G.; Sperb, R.; Smith, P. E.; van Gunsteren, W. F. *J. Chem. Phys.* **1995**, *102*, 5451−5459.
(55) Hub, J. S.; Groot, B. L.; Grubmüller, H.; Groenhof, G. *J. Chem. Theory Comput.* **2014**, *10*, 381−390.
(56) McLaughlin, S. *Annu. Rev. Biophys. Bio. Chem.* **1989**, *18*, 113−136.
(57) Frisch, M. J. et al. *Gaussian 03*, Revision C.02; Gaussian, Inc.: Wallingford, CT, 2004.
(58) Bayly, C.; Cieplak, P.; Cornell, W.; Kollman, P. *J. Phys. Chem.* **1993**, *97*, 10269−10280.
(59) Schmid, N.; Eichenberger, A.; Choutko, A.; Riniker, S.; Winger, M.; Mark, A.; Van Gunsteren, W. *Eur. Biophys. J.* **2011**, *40*, 843−856.
(60) Baptista, A. M.; Teixeira, V. H.; Soares, C. M. *J. Chem. Phys.* **2002**, *117*, 4184−4200.
(61) Machuqueiro, M.; Baptista, A. M. *J. Phys. Chem. B* **2006**, *110*, 2927−2933.
(62) van der Spoel, D.; Lindahl, E.; Hess, B.; Groenhof, G.; Mark, A. E.; Berendsen, H. J. C. *J. Comput. Chem.* **2005**, *26*, 1701−1718.
(63) Hess, B.; Kutzner, C.; van der Spoel, D.; Lindahl, E. *J. Chem. Theory Comput.* **2008**, *4*, 435−447.
(64) Reif, M. M.; Hünenberger, P. H. *J. Chem. Phys.* **2011**, *134*, 144104.
(65) Hermans, J.; Berendsen, H. J. C.; van Gunsteren, W. F.; Postma, J. P. M. *Biopolymers* **1984**, *23*, 1513−1518.
(66) Hess, B. *J. Chem. Theory Comput.* **2008**, *4*, 116−122.
(67) Miyamoto, S.; Kollman, P. *J. Comput. Chem.* **1992**, *13*, 952−962.
(68) Bussi, G.; Donadio, D.; Parrinello, M. *J. Chem. Phys.* **2007**, *126*, 014101.
(69) Berendsen, H. J. C.; Postma, J. P. M.; van Gunsteren, W. F.; DiNola, A.; Haak, J. R. *J. Chem. Phys.* **1984**, *81*, 3684−3690.
(70) Smith, P. E.; van Gunsteren, W. F. *J. Chem. Phys.* **1994**, *100*, 3169−3174.
(71) Rocchia, W.; Sridharan, S.; Nicholls, A.; Alexov, E.; Chiabrera, A.; Honig, B. *J. Comput. Chem.* **2002**, *23*, 128−137.
(72) Li, L.; Li, C.; Sarkar, S.; Zhang, J.; Witham, S.; Zhang, Z.; Wang, L.; Smith, N.; Petukh, M.; Alexov, E. *BMC Biophys.* **2012**, *5*, 9.
(73) Gilson, M.; Sharp, K.; Honig, B. *J. Comput. Chem.* **1987**, *9*, 327−335.
(74) Kumler, W.; Eiler, J. J. *J. Am. Chem. Soc.* **1943**, *65*, 2355−2361.
(75) Lee, F. S.; Chu, Z. T.; Warshel, A. *J. Comput. Chem.* **1993**, *14*, 161−185.
(76) Eberini, I.; Baptista, A.; Gianazza, E.; Fraternali, F.; Beringhelli, T. *Proteins Struct. Funct. Bioinf.* **2004**, *54*, 744−758.
(77) Warshel, A. *Annu. Rev. Biophys. Bio. Chem.* **1991**, *20*, 267−298.
(78) Martel, P.; Baptista, A.; Petersen, S. *Biotechnol. Annu. Rev.* **1996**, *2*, 315−372.
(79) Schutz, C. N.; Warshel, A. *Proteins: Struct. Funct. Genet.* **2001**, *44*, 400−417.
(80) Teixeira, V. H.; Cunha, C. C.; Machuqueiro, M.; Oliveira, A. S. F.; Victor, B. L.; Soares, C. M.; Baptista, A. M. *J. Phys. Chem. B* **2005**, *109*, 14691−14706.
(81) Machuqueiro, M.; Campos, S. R. R.; Soares, C. M.; Baptista, A. M. *J. Phys. Chem. B* **2010**, *114*, 11659−11667.

(82) Baptista, A. M.; Soares, C. M. *J. Phys. Chem. B* **2001**, *105*, 293−309.
(83) Allen, M.; Tildesley, D. *Computer Simulation of Liquids*; Oxford University Press: USA, 1987; pp 191−198.
(84) Kučerka, N.; Nieh, M.-P.; Katsaras, J. *Biochem. Biophys. Acta, Biomembr.* **2011**, *1808*, 2761−2771.
(85) Knecht, V.; Klasczyk, B. *Biophys. J.* **2013**, *104*, 818.
(86) Börjesson, U.; Hünenberger, P. H. *J. Chem. Phys.* **2001**, *114*, 9706.
(87) Burgi, R.; Kollman, P. A.; van Gunsteren, W. F. *Proteins Struct. Funct. Bioinf.* **2002**, *47*, 469−480.
(88) Dlugosz, M.; Antosiewicz, J. M. *Chem. Phys.* **2004**, *302*, 161−170.
(89) Dlugosz, M.; Antosiewicz, J. M.; Robertson, A. D. *Phys. Rev. E* **2004**, 69.
(90) Lee, M. S.; Salsbury, F. R.; Brooks, C. L. *Proteins Struct. Funct. Bioinf.* **2004**, *56*, 738−752.
(91) Mongan, J.; Case, D. A.; McCammon, J. A. *J. Comput. Chem.* **2004**, *25*, 2038−2048.
(92) Machuqueiro, M.; Baptista, A. M. *Biophys. J.* **2007**, *92*, 1836−1845.
(93) Stern, H. A. *J. Chem. Phys.* **2007**, *126*, 164112.
(94) Machuqueiro, M.; Baptista, A. M. *Proteins Struct. Funct. Bioinf.* **2008**, *72*, 289−298.
(95) Campos, S. R. R.; Baptista, A. M. *J. Phys. Chem. B* **2009**, *113*, 15989−16001.
(96) Machuqueiro, M.; Baptista, A. M. *J. Am. Chem. Soc.* **2009**, *131*, 12586−12594.
(97) Campos, S. R. R.; Machuqueiro, M.; Baptista, A. M. *J. Phys. Chem. B* **2010**, *114*, 12692−12700.
(98) Machuqueiro, M.; Baptista, A. M. *Proteins Struct. Funct. Bioinf.* **2011**, *79*, 3437−3447.
(99) Vorobjev, Y. N. *J. Comput. Chem.* **2012**, *33*, 832−842.
(100) Vila-Viçosa, D.; Campos, S. R. R.; Baptista, A. M.; Machuqueiro, M. *J. Phys. Chem. B* **2012**, *116*, 8812−8821.
(101) Wallace, J. A.; Shen, J. K. *J. Chem. Phys.* **2012**, *137*, 184105.
(102) Morrow, B.; Koenig, P.; Shen, J. *J. Chem. Phys.* **2012**, *137*, 194902−194902.
(103) Henriques, J.; Costa, P. J.; Calhorda, M. J.; Machuqueiro, M. *J. Phys. Chem. B* **2013**, *117*, 70−82.
(104) Carvalheda, C. A.; Campos, S. R.; Machuqueiro, M.; Baptista, A. M. *J. Chem. Inf. Model.* **2013**, *53*, 2979−2989.
(105) Vila-Viçosa, D.; Teixeira, V. H.; Santos, H. A. F.; Machuqueiro, M. *J. Phys. Chem. B* **2013**, *117*, 7507−7517.